
NeuSym-HLS: Learning-Driven Symbolic Distillation in High-Level Synthesis of Hardware Accelerators

Chung-Mou Pan, Salma Elmalaki, Yasser Shoukry, Sitaoh Huang

Department of Electrical Engineering and Computer Science

University of California, Irvine

Irvine, CA 92697

{chungmop, selmalak, yshoukry, sitaoh}@uci.edu

Abstract

1 Domain-specific hardware accelerators for deep neural network (DNN) inference
2 have been widely adopted. Traditional DNN compression techniques such as
3 pruning and quantization help but can fall short when aggressive hardware effi-
4 ciency is required. We present *NeuSym-HLS*, a partial symbolic distillation and
5 high-level hardware synthesis flow to compress and accelerate DNN inference for
6 edge computing. NeuSym-HLS replaces a portion of the layers of a trained DNN
7 model with compact analytic expressions obtained via symbolic regression, and
8 generates efficient hardware accelerators. The resulting hardware accelerator of the
9 hybrid DNN-symbolic model provides well balanced performance in algorithmic
10 accuracy, hardware resource, and inference latency. Our evaluation on vision tasks
11 showed that NeuSym-HLS reduces hardware resource usage, reduces latency, while
12 maintaining model inference accuracy.

13

1 Introduction

14 Deep neural networks (DNNs) have been widely adopted in a wide range of application domains.
15 Despite their significant accuracy performance, DNN models require intensive computation, and
16 they often lack explainability, which poses risks for certain applications and systems like real-time
17 systems and cyber-physical systems. To improve DNN’s computational performance, researchers
18 have proposed various solutions at both the model architecture level and the computing system
19 level, including model compression techniques and domain-specific acceleration with application-
20 specific integrated circuits (ASICs) and field-programmable gate arrays (FPGAs). Model compression
21 and hardware acceleration techniques often need to be applied together with specialized hardware
22 architecture and DNN retraining to gain computing efficiency and maintain model accuracy.

23 Compared to the computational challenges discussed above, the explainability of DNN-based machine
24 learning models is an even harder problem and is more serious in certain domains that require rigorous
25 robustness and verification standard. In recent years, researchers have proposed techniques aiming to
26 create interpretable versions of DNN-based models. Symbolic regression (SR) has become one of
27 the popular techniques and has been shown to be able to replace some DNN models without much
28 accuracy degradation.

29 To address the computation and explainability challenges in DNN-based models, we propose *NeuSym-*
30 *HLS*, a DNN model compression and hardware accelerator generation framework that performs co-
31 optimization of DNN model compression and high-level synthesis (HLS) based hardware architecture
32 design space exploration. Our proposed NeuSym-HLS flow features three key components, including
33 (i) *partial symbolic distillation* and quantization pass that compresses given DNN models by replacing
34 computational heavy layers with symbolic expressions; (ii) hardware-aware design space exploration
35 of *symbolic operation selection*; and (iii) *symbolic-architecture co-design* engine which finetune the

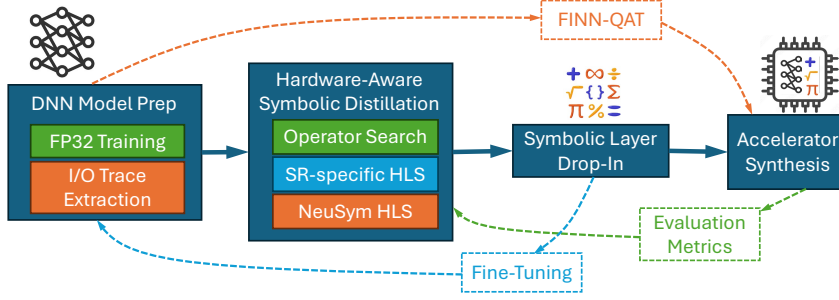


Figure 1: NeuSym-HLS Overview. FP32 training produces an activation trace that feeds hardware-aware symbolic regression (SR). The resulting analytic layer is *dropped-in* and the hybrid design synthesized. Optional branches (blue dashed boxes/paths) support QAT and post-SR fine-tuning.

36 symbolic distilled model and generates efficient hardware accelerator design via high-level synthesis
 37 (HLS). NeuSym-HLS significantly reduces hardware resource usage and inference latency of DNN
 38 models accelerators, while delivering near-original inference accuracy.

39 2 Background and Related Works

40 Deep learning (DL) inference on hardware accelerators hinges on two orthogonal themes: *(i)*
 41 *hardware-aware design flows* that translate high-level specifications (e.g., DNN models and C/C++
 42 implementations) into efficient RTL designs, and *(ii)* *model-compression techniques* that shrink model
 43 size without sacrificing accuracy. We review the state-of-the-art techniques in both areas before
 44 introducing our NeuSym-HLS flow.

45 **High-Level Synthesis of Hardware Accelerators.** Modern tools such as AMD Vitis HLS let
 46 developers express kernels in C/C++ and refine them with HLS pragmas (e.g. dataflow, pipeline)
 47 to guide HLS compiler to optimize hardware designs and meet tight latency and resource utilization
 48 targets on FPGAs or ASICs [1]. Dozens of works show that careful loop unrolling, tiling, and
 49 memory partitioning can deliver real-time CNN inference even on low-power resource-constrained
 50 devices [2, 3].

51 **Symbolic Regression and Hardware Acceleration.** Tsoi et al. [4] introduce FPGA-resident sym-
 52 bolic regression (SR) accelerators that entirely replace dataset-level inference with compact analytic
 53 expressions, achieving sub- μ s latency on physics workloads. Later, SymbolNet [5] bridges this idea
 54 with DNNs by combining neural symbolic regression with adaptive dynamic pruning to achieve
 55 efficient model compression, enabling low-latency inference even for high-dimensional datasets on
 56 FPGA hardware.

57 **Challenges in Scaling Symbolic Regression.** Differentiable Genetic Programming (DGP) [6] tackles
 58 the high-dimensional SR problem by relaxing tree structures into continuous representations. Even
 59 so, the authors note that discovering compact formulas for thousands of features remains expensive,
 60 confirming that “all-layer” SR on deep networks is impractical.

61 3 NeuSym-HLS Framework

62 3.1 NeuSym-HLS Framework Overview

63 Figure 1 illustrates the end-to-end **NeuSym-HLS** flow, starting from a floating-point PyTorch model
 64 and ending with post-synthesis metrics. Solid arrows represent the default path; dashed arrows
 65 represent optional branches such as quantization-aware training (QAT) and end-to-end fine-tuning of
 66 the neural-symbolic hybrid network.

67 **Hardware-Aware Symbolic Regression (SR).** For each of the N output channels fit an analytic
 68 function

$$\ell_j = f_j(\mathbf{h}) \quad \text{with} \quad f_j \in \text{SR}(\mathcal{O}, C_{\max}),$$

69 where \mathcal{O} is the operator set (e.g., $\{+, -, *, \sin, \exp\}$) and C_{\max} a complexity budget.

Table 1: Example snapshot of symbolic regression Hall of Fame produced by PySR.

Complexity	Loss	Equation
1	1926.54	0.7614
3	0.4929	$x_1 \cdot x_1$
5	0.4835	$(x_1 \cdot x_1) \cdot 0.9978$
6	1.10×10^{-11}	$\sin(x_0) + x_1^2$
13	9.88×10^{-12}	$x_1^2 + \sin(x_0 + \cos((x_1 - x_1) - \frac{\pi}{2}))$

Table 2: Evaluating Generated Accelerators on the MNIST Task

Model ID	Acc (%)	Latency	LUT (%)	FF (%)	DSP (%)
BL-MLP	96.4	106k	21k (41%)	44k (41%)	976 (443%)
SR-MLP	94.4	110k	9,499 (17%)	6,833 (6%)	96 (43%)
Q-MLP	96.3	158	1,347 (3%)	1,955 (2%)	0 (0%)
Q-SR-MLP	95.8	75	982 (2%)	1,645 (2%)	0 (0%)
BL-LeNet	98.4	130k	602k (1,132%)	435k (408%)	2,769 (1,258%)
SR-LeNet	99.0	130k	395k (743%)	256k (241%)	2,194 (997%)
Q-LeNet	97.7	8,810	7,173 (13%)	10k (10%)	0 (0%)
Q-SR-LeNet	96.2	35k	3,146 (6%)	3,576 (3%)	0 (0%)
SR Paper[4]	85.3	13 ¹	7,592 (14%)	6,424 (6%)	160 (73%)

70 The equation with the lowest validation loss under the complexity threshold (e.g., Entry #13) is
 71 selected for deployment. This expression is translated into synthesizable HLS C code for hardware
 72 integration, as shown in Listing 1.

```

73 float fc3_symbolic(float x0, float x1) {
74     // (x1 * x1) + sin(x0 + cos((x1 - x1) - 1.5707971f))
75     #pragma HLS INLINE
76     float term1 = x1 * x1;
77     float term2 = sinf(x0 + cosf((x1 - x1) - 1.5707971f));
78     return term1 + term2;
79 }
80 }
```

Listing 1: Auto-generated HLS C implementation of Entry #13

82 3.2 Hardware-Aware Symbolic Regression in NeuSym-HLS

83 NeuSym-HLS builds on **PySR** [7], an open-source symbolic regression library for discovering
 84 human-interpretable equations through a high-performance Genetic Programming approach with
 85 its unique evolve–simplify–optimize loop algorithm, but enhances its fitness metric to account for
 86 hardware-aware trade-offs, including *inference latency* and *FPGA resource utilization*. This section
 87 details the two key design dimensions that must be fixed *before* large-scale symbolic regression:
 88 **Search-space definition:** selecting unary/binary operator sets that offer the best balance between
 89 interpretability and synthesis overhead (Section A). **Distillation placement** — deciding which DNN
 90 layers to be replaced by symbolic expressions to optimize synthesis metrics while preserving accuracy
 91 (Section B).

92 4 Evaluation Results and Analysis

93 Our evaluation setup is explained in Appendix C.

94 TABLE 2 and TABLE 3 summarized all the evaluation results on MNIST task and SVHN task,
 95 respectively. According to the evaluation results shown in these two tables, NeuSym-HLS generated
 96 compressed models and accelerators (names start with “SR-” or “Q-”) achieve more performance and
 97 resource efficient hardware acceleration compared to baseline implementations, while maintaining
 98 high accuracy. When compared against state-of-the-art works, NeuSym-HLS achieves much higher
 99 accuracy while using much less resource, and having similar levels of latency.

Table 3: Evaluating Generated Accelerators on the SVHN Task

Model ID	Acc (%)	Latency	LUT (%)	FF (%)	DSP (%)
BL-MLP	94.1	12.6m	4,665 (8%)	3,182 (2%)	15 (6%)
SR-1L-SCE	97.7	18.4m	5,598 (10%)	3,316 (3%)	16 (7%)
SR-1L-SRL	97.6	18.4m	2,969 (5%)	1,693 (1%)	7 (3%)
SR-1L-POL	98.2	18.4m	2,894 (5%)	1,630 (1%)	7 (3%)
SR-2L-SCE	90.3	12.6m	7,803 (14%)	4,662 (4%)	23 (10%)
SR-2L-SRL	91.8	12.6m	4,089 (7%)	2,555 (2%)	7 (3%)
SR-2L-POL	90.7	12.6m	3,627 (6%)	2,353 (2%)	5 (2%)
Q-MLP	93.9	8,737	48,357 (90%)	32,367 (30%)	0 (0%)
Q-SR-1L-SCE	91.7	65,550	45,682 (86%)	14,287 (13%)	0 (0%)
Q-SR-1L-SRL	93.9	65,550	46,289 (87%)	14,368 (13%)	0 (0%)
Q-SR-1L-POL	90.9	65,550	45,661 (86%)	14,291 (13%)	0 (0%)
SymbolNet [5]	94	520 ¹	27,407 (52%)	16,286 (15%)	77 (35%)

100 **Operator-Set Search: Identifying Key Unary Functions.** We explore the design space of operator
 101 selection for symbolic regression (SR) to identify the most efficient combinations of operators. As
 102 discussed in Section A, we defined non-trig and trig-enriched sets of operators. Fig. 3 and Fig. 4
 103 present the losses (the lower the better) of varies combinations of SR operators. According to the
 104 figures, trig-enriched unary operator sets tend to perform better than the non-trig operator sets. From
 105 Fig. 4, We can also observe that better performing non-trig operator sets consistently include “ReLU”
 106 operator.

107 **Impact of Operator Selection on Hardware Accelerators.** We selected various representative
 108 combinations of SR operators, and use them to approximate the *entire* DNN model, and evaluate
 109 the performance of generated hardware accelerators. Fig. 2 shows the evaluation results. When
 110 running symbolic regression on the whole DNN model, the hardware usage decreases significantly,
 111 however, the accuracy also drops significantly to 72%. This supports our motivation of doing **partial**
 112 symbolic distillation instead of full model symbolic approximation. Besides, different combinations
 113 of operators lead to different results of accuracy, hardware resource usage, and latency, therefore, the
 114 operator selection search in NeuSym-HLS is essential to generate efficient accelerator.

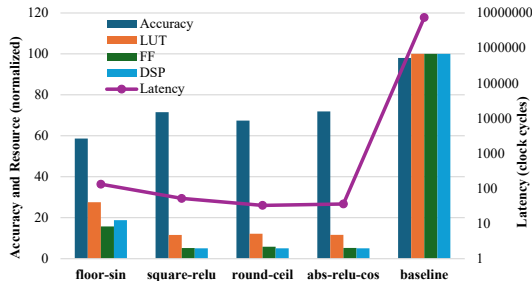


Figure 2: Comparing Symbolic Regression Operator Combinations on the Area and the Performance of Hardware Accelerators for LeNet (MNIST Task).

115 5 Conclusion

116 NeuSym-HLS bridges the gap between the efficiency of aggressive quantization and the interpretability
 117 of full-network symbolic regression. By selectively distilling the final layer(s) of a neural network
 118 into compact symbolic expressions, leveraging quantization-aware training and other standard com-
 119 pression techniques, our results demonstrate that symbolic distillation is especially advantageous
 120 for low-dimensional and high-latency output layers. Meanwhile, quantization remains an effective
 121 tool for compressing the remaining network, underscoring the complementary strengths of both
 122 approaches for resource-efficient and interpretable DNN deployment.

¹Reported latency from [4] and [5] reflects only HLS kernel latency using hls4ml, and does not include end-to-end design latency; actual deployment latency may be higher.

123 **References**

- 124 [1] Xilinx Inc. Vitis high-level synthesis user guide, 2022. https://www.xilinx.com/support/documents/sw_manuals/xilinx2022_2/ug1399-vitis-hls.pdf.
- 125
- 126 [2] Chen Zhang, Peng Li, Guangyu Sun, Yijin Guan, Bingjun Xiao, and Jason Cong. Optimizing fpga-based
127 accelerator design for deep convolutional neural networks. In *Proceedings of the 2015 ACM/SIGDA
128 International Symposium on Field-Programmable Gate Arrays*, pages 161–170, 2015.
- 129 [3] Stylianos I Venieris and Christos-Savvas Bouganis. fpgaconvnet: A framework for mapping convolutional
130 neural networks on fpgas. In *2016 IEEE 24th Annual International Symposium on Field-Programmable
131 Custom Computing Machines (FCCM)*, pages 40–47, 2016.
- 132 [4] Ho Fung Tsoi, Adrian Alan Pol, Vladimir Loncar, Ekaterina Govorkova, Miles Cranmer, Sridhara Dasu,
133 Peter Elmer, Philip Harris, Isobel Ojalvo, and Maurizio Pierini. Symbolic regression on fpgas for fast
134 machine learning inference. In *EPJ Web of Conferences*, volume 295, page 09036, 2024.
- 135 [5] Ho Fung Tsoi, Vladimir Loncar, Sridhara Dasu, and Philip Harris. SymbolNet: Neural Symbolic Re-
136 gression with Adaptive Dynamic Pruning for Compression. *Machine Learning: Science and Technology*,
137 6(1):015021, 2025.
- 138 [6] Peng Zeng, Xiaotian Song, Andrew Lensen, Yuwei Ou, Yanan Sun, Mengjie Zhang, and Jiancheng Lv.
139 Differentiable genetic programming for high-dimensional symbolic regression, 2023.
- 140 [7] Miles Cranmer. Interpretable machine learning for science with pysr and symbolicregression.jl. *arXiv
141 preprint arXiv:2305.01582*, 2023.
- 142 [8] Xavier Glorot, Antoine Bordes, and Yoshua Bengio. Deep sparse rectifier neural networks. In *Proceedings
143 of the Fourteenth International Conference on Artificial Intelligence and Statistics*, pages 315–323, 2011.
- 144 [9] Yaman Umuroglu, Nicholas J. Fraser, Giulio Gambardella, Michaela Blott, Philip Leong, Magnus Jahre,
145 and Kees Vissers. Finn: A framework for fast, scalable binarized neural network inference. In *Proceedings
146 of the 2017 ACM/SIGDA International Symposium on Field-Programmable Gate Arrays*, FPGA ’17, pages
147 65–74. ACM, 2017.
- 148 [10] Marco Virgolin and Solon P. Pissis. Symbolic regression is np-hard. *arXiv preprint arXiv:2207.01018*,
149 2022.

150 Appendices

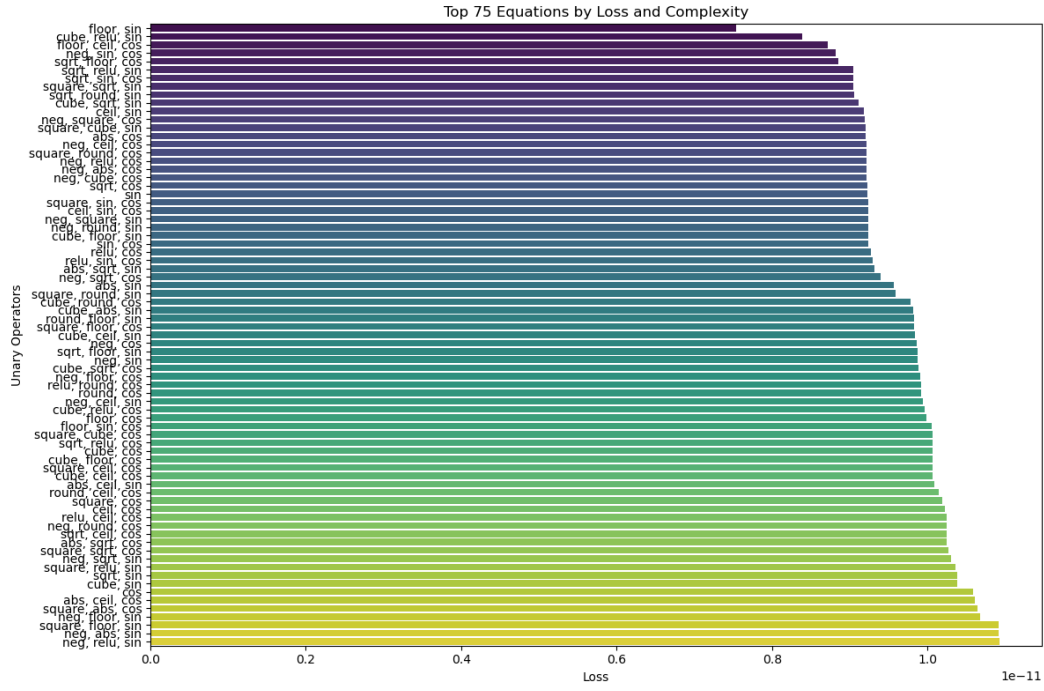


Figure 3: Top 75 trig-enriched operator combinations, sorted by loss.

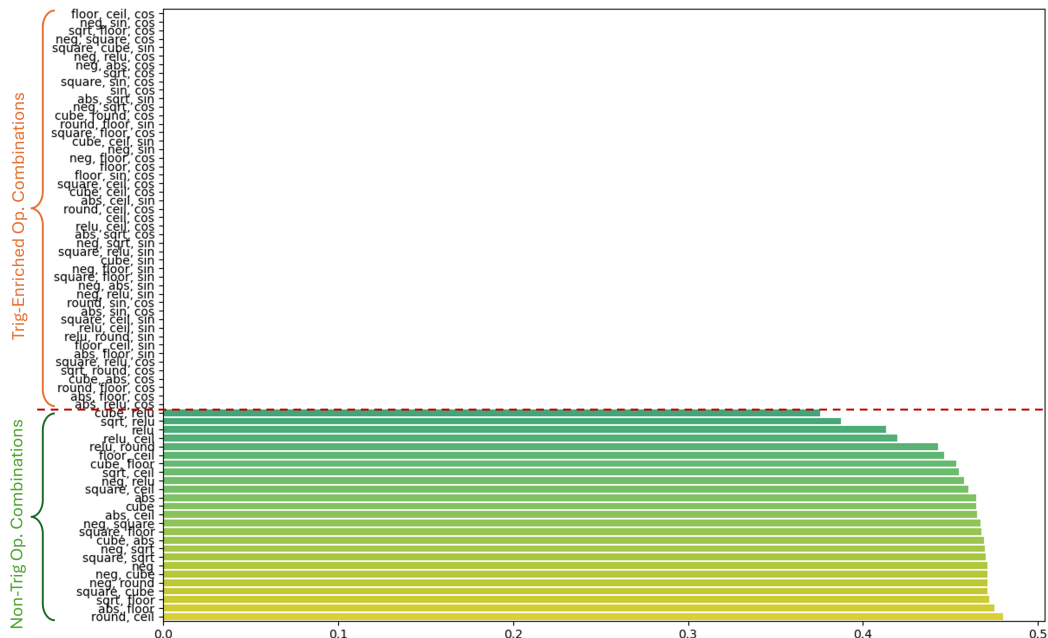


Figure 4: Trig-enriched (top) vs. Non-trig (bottom) operator combinations.

151 **A Operator-Set Study**

152 A preliminary sweep determined which unary functions should enter the search space. To system-
153 atically explore the symbolic design space before scaling to full DNN regression, we constructed
154 a synthetic $2 \rightarrow 1$ regression task ($\mathbf{x} \in \mathbb{R}^2 \mapsto y$) whose ground-truth function blends polynomial
155 and sinusoidal terms. This task serves as a proxy to mirror the kinds of nonlinearities seen in neural
156 networks, allowing us to evaluate how different operator combinations in PySR navigate the trade-off
157 between interpretability and accuracy. Two broad categories of unary operators were explored:

- 158 1. **Non-trig:** {neg, square, cube, abs, sqrt, relu, round, floor, ceil, sign}
159 2. **Trig-enriched:** all of the non-trig plus {sin, cos}

160 We swept through the space of all valid 3-element and 2-element subsets of candidate unary operators
161 (i.e., $\binom{|\mathcal{F}|}{3} + \binom{|\mathcal{F}|}{2}$), where \mathcal{F} is the operator pool). For each subset, we trained a PYSRREGRESSOR
162 using the fixed binary operator set $\{+, -, *\}$, with 40 iterations and 10 independent populations.

163 The **trig-enriched** subsets consistently achieved validation losses around $\mathcal{L}_2 \approx 10^{-11}$, while the
164 best-performing **non-trig** configuration (square + relu) stalled at approximately $\mathcal{L}_2 \approx 10^{-1}$. Hence,
165 even under identical tree-depth and complexity budgets, incorporating sin/cos closes a ~ 5 -order-of-
166 magnitude accuracy gap. Within the non-trig family, sets that retained relu always outperformed
167 those that did not, which aligns with prior findings on ReLU’s effectiveness in deep neural network
168 training [8].

169 Guided by these findings, we designed three sets of operators to be used in the NeuSym-HLS
170 framework, to meet various model compression and accelerator optimization needs.

- 171 1. **SCE (Sin–Cos–Exp):** $\{+, -, *, \sin, \cos, \exp\}$ – highest expressiveness; used when accuracy
172 is paramount.
173 2. **SRL (Square–ReLU):** $\{+, -, *, \text{square}, \text{relu}\}$ – no trig; captures piece-wise linearity with
174 good hardware efficiency.
175 3. **POL (Polynomial):** $\{+, -, *, /\}$ – pure arithmetic baseline.

176 **B Distillation Strategy**

177 Symbolic regression is appealing for interpretability, yet GP-based methods scale poorly to high-
178 dimensional data because their stochastic, discrete tree search lacks gradient guidance [6].

179 Our LeNet study confirms this: turning the whole network into one symbolic expression either failed
180 to converge or produced unwieldy formulas, dropping accuracy from 98% to $\approx 70\%$. Full-network
181 symbolic distillation is hence impractical for high-dimensional vision data.

182 To mitigate this, we adopt a targeted distillation strategy. Rather than distilling the entire network,
183 we identify specific layers or submodules where symbolic expressions can be injected with min-
184 imal impact on end-to-end accuracy. Criteria for selection include **computational intensity** and
185 **input/output dimensionality** of the layer (low-dimensional layers preferred). We therefore tested
186 symbolic replacement of the final one or two dense layers, with the detailed accuracy–resource
187 trade-off reported in TABLE 3.

188 **C Evaluation Setup**

189 **DNN Models and Tasks.** We evaluate our proposed NeuSym-HLS framework on three DNNs across
190 two tasks, as shown in TABLE 4. These DNNs vary layer types, number of layers, and number of
191 neurons in the layers.

192 **Model Training and Quantization.** All DNN models are first trained with standard cross-entropy
193 loss for 10 epochs (Adam, learning rate $1e-3$, batch size 64). In some evaluations, the model goes
194 through quantization-aware training (QAT) using FINN [9] as well as fine-tuning, where each network
195 is fine-tuned for 5 epochs using 2-bit activations and weights.

Table 4: Neural Network Benchmarks Used in This Study

Task & Model	DNN Architecture Details (# of layers and neurons)
MNIST MLP	Input: $784 \rightarrow 128 \rightarrow 64 \rightarrow 10$ output classes
MNIST LeNet	Two conv-pool blocks ($6 \times 5 \times 5$ and $16 \times 5 \times 5$ kernels, 2×2 max-pool), followed by $120 \times 5 \times 5$ conv and one FC-10 output layer
SVHN MLP	Input: $3072 \rightarrow 512 \rightarrow 128 \rightarrow 1$ (binary; digits “1” vs “7”)

196 **Symbolic Regression Engine.** We leverage an open-source tool, PySR [7], to build the symbolic
 197 regression engine inside NeuSym-HLS. We use PySR v1.5.0¹ where search parameters $n_{\text{iterations}}$
 198 and populations are set to 40 and 10 respectively. NeuSym-HLS framework explores the non-linear
 199 operator selection space on top of a combination of *POLY*, *SCE*, and *SRL* operator sets. The default
 200 ℓ_2 regression loss on DNN layer logits is used.

201 **Hardware Accelerator Prototyping Platform.** We use an AMD XC7Z020 FPGA (Zynq-7000 series)
 202 as our hardware accelerator prototyping and evaluation platform. We use Vitis HLS (v2022.2) [1]
 203 to generate hardware designs, and target 100 MHz clock rate in the synthesis (post-place and route
 204 timing met in all designs).

205 **Evaluation Metrics.** We evaluate the effectiveness of NeuSym-HLS with three metrics, (i) inference
 206 **accuracy (%)** of compressed DNN model on the full validation set; (ii) inference **latency** (in clock
 207 cycles and in microseconds at 100 MHz) of generated hardware accelerator; (iii) **resource usage** of
 208 generated hardware accelerator on FPGA, including look-up table (LUT), flip-flop (FF), and DSP
 209 counts, expressed both in absolute numbers and as utilization percentage of the targeting FPGA
 210 device capacity.

211 We present end-to-end hardware synthesis results that answer three experimental questions:

- 212 1. **Operator relevance.** Which *unary* operators matter most for symbolic regression on image
 213 data?
- 214 2. **Pure-SR feasibility.** How well can a *fully* symbolic model approximate MNIST without
 215 any MACs?
- 216 3. **Hybrid efficiency.** When only the cost-critical layers of a DNN are replaced by symbolic
 217 expressions, how do accuracy, latency, and FPGA utilization compare with floating-point
 218 and quantized baselines?

219 To answer these, the section proceeds in five steps:

- 220 • *Operator-set search.* A 220-way grid sweep identifies *square+relu* as the most accurate
 221 non-trigonometric set and confirms the importance of keeping *relu*.
- 222 • *End-to-end SR on MNIST.* We train a pure symbolic regressor on the full dataset and report
 223 accuracy and resource cost against BL-MLP and Q-MLP baselines.
- 224 • *LeNet-5 hybrid on MNIST.* Replacing only the final fully connected layer with a symbolic
 225 expression (NeuSym-HLS) cuts LUT, FF, and DSP usage by up to $3.3\times$ at iso-accuracy and
 226 reduces latency by $1.5\times$.
- 227 • *Fully-connected MLP.* The same partial-distillation recipe is applied to a three-layer MLP,
 228 showing that gains generalize beyond convolutional architectures.
- 229 • *Same experiments on another SVHN Dataset.* Expanded SVHN experiments which include
 230 two-layer replacement and alternative operator sets.

231 **Model ID Naming Scheme:** BL = baseline (floating-point, no symbolic or quantization); SR =
 232 symbolic regression (last layer(s) replaced); Q = quantized (QAT, 2-bit weights, no symbolic); Q-SR =
 233 quantized + symbolic regression; 1L/2L = number of layers replaced; SCE, SRL, POL = operator sets
 234 (see Sec. A).

¹<https://github.com/MilesCranmer/PySR>

235 **D NeuSym-HLS on MNIST: A Generality Study**

236 To evaluate the effectiveness and generality of our NeuSym-HLS symbolic distillation approach, we
 237 apply NeuSym-HLS to a fully connected multilayer perceptron (MLP) and a LeNet model trained on
 238 MNIST task. Fig. 5 shows the evaluation results for the MLP model.

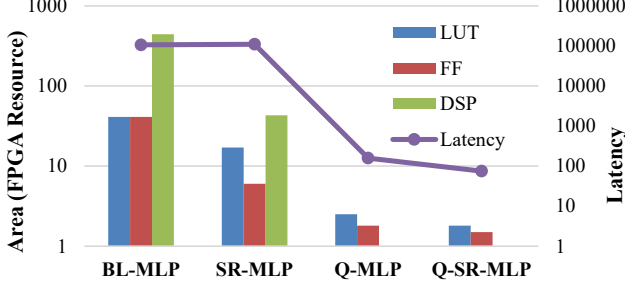


Figure 5: Hardware Accelerators for MLP Model on the MNIST Task.

239 The Q-SR-MLP version delivers the most aggressive compression while still preserving accuracy.
 240 Compared to SR-MLP, the Q-SR-MLP variant reduces latency by more than an order of magnitude and
 241 lowers LUT/FF usage to under 1% of the original baseline. These results confirm that NeuSym-HLS
 242 works effectively: symbolic final-layer replacement consistently reduces hardware cost, when applied
 243 to either convolutional models or MLPs.

244 **D.1 SVHN Binary Classifier: Depth and Operator-Set Exploration**

245 We now evaluate NeuSym-HLS on the SVHN dataset using a compact binary classifier architecture.
 246 Our analysis explores two axes: (1) the depth of symbolic replacement—whether 1 or 2 layers are
 247 replaced—and (2) the symbolic operator family used.

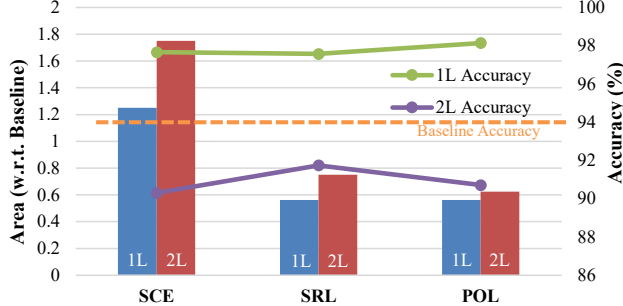


Figure 6: 1-layer vs. 2-layer Symbolic Distillation, in Area and Accuracy.

248 Fig. 6 shows the evaluation results. Among various versions, SR-1L-POL achieves the highest
 249 accuracy (98.2%) while maintaining the lowest LUT usage (5%). SR-1L-SRL trails slightly at 97.6%
 250 but with nearly identical hardware usage, whereas SR-1L-SCE lags in both accuracy and LUT cost.
 251 This confirms that operator set selection has a tangible impact on hardware efficiency. SCE incurs the
 252 highest DSP cost at 6.8%, while SRL and POL remain below 3%.

253 We next examine the effect of replacing two layers instead of one. Evaluation results show that
 254 2-layer symbolic models consistently degrade in accuracy across all operator families. For instance,
 255 accuracy drops by 7.4 points for SCE and 6.9 points for POL compared to their 1-layer counterparts.
 256 Resource costs also increase, confirming that aggressive symbolic replacement compromises both
 257 accuracy and efficiency.

258 Finally, TABLE 3 presents detailed synthesis metrics for all designs. NeuSym-HLS achieves better
 259 accuracy than both the quantized baseline (Q-MLP) and prior SR accelerators (e.g., SR-Paper [5])
 260 while reducing LUT and DSP usage by over 10× in some configurations. Notably, Q-SR-1L-POL
 261 matches the performance of SR-1L-POL but executes in just 65k cycles, enabling low-latency
 262 inference without multipliers.

263 These results confirm that symbolic regression is most effective when applied selectively and targeting
264 a single output layer using low-complexity, hardware-friendly operators.

265 E Discussion and Future Work

266 E.1 Resource–Latency Trade-offs

267 Our results demonstrate that even replacing a **single fully connected layer** with a symbolic expression
268 preserves accuracy within 1% of the floating-point baseline while reducing LUT and flip-flop usage
269 by an order of magnitude and eliminating almost all DSP requirements (Tables 2, 3). Quantization
270 excels at raw speed, achieving up to $675 \times$ latency reductions on MNIST, but can inflate logic usage
271 on larger inputs (e.g., 90% LUT for SVHN). On SVHN, symbolic regression alone can offer the best
272 Pareto trade-off: SR-1L-POL achieves 98.2% accuracy with only 5% LUT and 7% DSP, surpassing
273 both baseline and quantized variants. Combining QAT with symbolic regression (Q-SR) is most
274 beneficial for small networks (e.g., MNIST MLP), but provides diminishing returns for deeper
275 architectures due to accumulator overhead. For example, on MNIST, quantized symbolic models
276 achieve up to 98% LUT savings relative to the baseline with less than 1% drop in accuracy. On
277 SVHN, replacing one layer with symbolic expressions delivers strong accuracy-resource trade-offs,
278 while two-layer replacements begin to significantly degrade accuracy, highlighting a practical limit to
279 symbolic compression depth.

280 E.2 Operator Set and Depth Ablations

281 Our operator-set ablation shows that the polynomial-only (POL) search yields the best balance of
282 accuracy and DSP cost. Depth ablation confirms that symbolic regression is most effective for the last,
283 low-dimensional layers; replacing multiple layers can halve logic again, but with up to 8 percentage
284 points accuracy drop, indicating diminishing returns for high-dimensional layers.

285 E.3 Current Limitations

286 Some practical limitations remain. Currently, symbolic partitioning and formula integration require
287 manual intervention (copy-pasting PySR outputs, editing typecasts), which can be streamlined. Also,
288 symbolic regression search can be computationally intensive, particularly as the number of candidate
289 operators or target layers and dimensions increase. This is expected, as the search space for equations
290 grows combinatorially with the number of available parameters. Recent work formally proves that
291 symbolic regression is an NP-hard problem [10], confirming the intractability of exact solutions in
292 general cases. Finally, while symbolic methods are effective for fully connected layers, direct support
293 for convolutional and high-dimensional layers remains an open challenge.

294 E.4 Future Work

295 To further improve applicability and automation, future directions include: **Automated partition**
296 **selection:** Heuristics or learning-based methods to choose layers that yield optimal trade-offs. **CNN**
297 **layer support:** Extending symbolic regression to convolutional or depth-wise layers, possibly by
298 constraining expression growth. **Operator Complexity Study:** An algorithm to learn hardware-
299 specific cost models (latency and resource) for each operator type, and adaptively promote or demote
300 operators during training so that the final expression set simultaneously minimizes resource cost and
301 maintains accuracy performance.